Estimation of the influence of cloudiness on the Earth observation from space through a gap in a cloudy field

V.V. Belov[1a, b], I.V. Kirnos[2a, b], M.V. Tarasenkov[3a, b]
[a]V. E. Zuev Institute of Atmospheric Optics SB RAS, 1 Academician Zuev Square, Tomsk 634055, Russia; [b]National Research Tomsk State University, 36 Lenin Prospect, Tomsk 634050, Russia

ABSTRACT

For atmospheric correction of satellite images, the problem is formulated to estimate the distance from a cloud at which its influence on the satellite image of the Earth surface can be neglected. The Monte Carlo method of conjugate trajectories is used. The gap radius in the field of continuous cloudiness at which the influence of the cloudy medium on the received signal intensity does not exceed 10 % is obtained. It is revealed that for the Lambert law of radiation reflection from the Earth surface, the curve of the dependence of the received signal intensity on the gap radius has a maximum caused by the opposite influence of light scattering by the cloudy medium and radiation reflection by the surface (adjacency effect). To further generalize the examined problem to a stochastic cloud field, the method of direct simulation of photon trajectories in a stochastic medium is compared with G. A. Titov's method of closed equations in the gap vicinity. A comparison is carried out with the model of the stochastic medium in the form of a *cloud field* of constant geometric thickness consisting of rectangular *clouds* whose boundaries are determined by the stationary Poisson flow of points. It is demonstrated that results of calculations can differ at most by 20–30 %; however, in some cases (for some sets of initial data), the difference for the entire region of cloud cover indices is within 7 %.
Keywords: remote sensing, Monte Carlo method, atmospheric correction, cloud field, statistical averaging of the radiative transfer equation, G.A.Titov's method of closed equations

1. INTRODUCTION

Observation of the Earth surface from space is an important part of monitoring of the state of agricultural vegetation and pastures, investigation of humidity and pollution of soils, control over landslide processes and deformations of the landscape, forest and peat fires, detection of ecological changes (including those in the atmosphere), etc. [1–9].

In all these cases without exception it should be born in mind that observations are carried out through the atmosphere that distorts the initial signal, often in the presence of considerable aerosol pollution or cloudiness. Therefore, the estimation of the influence of the atmosphere, in particular, of the presence of cloudiness, on the received light fluxes acquires great significance.

In this case, the problem of atmospheric correction of satellite images is the procedure necessary for reliable interpretation of satellite data. In the presence of optically dense cloud fields, the problem of atmospheric correction consists in elimination of these regions from the consideration, that is, construction of a cloud mask [10]. In the presence of translucent or broken cloudiness, the problem of atmospheric correction consists in taking into account the influence of these optical-geometrical conditions of observation. During observation of cloudless regions near cloud fields and in gaps between clouds, the cloud field influences the image, for example, of the Earth surface underlying the cloudless region. The present work is devoted to a solution of the last problem; moreover, we here focus on the problem of determining the distance from the cloud at which its influence on the satellite image can be neglected.

2. OBSERVATION THROUGH A GAP IN A HOMOGENEOUS CLOUD FIELD

The following problem formulation is suggested (Figs. 1 and 2). A homogeneous cloud layer is located over the flat Earth surface at altitudes in the range from h_{min} to h_{max}. In the cloud layer, there is a cylindrical gap. A satellite system operating at the wavelength λ observes through the gap at the zenith angle θ_{rec} to the vertical an element of the Earth surface situated under the center of the gap. The parallel flux of sun rays is incident on the upper atmospheric boundary

[1] belov@iao.ru
[2]ikirnos@sibmail.com
[3]tmv@iao.ru

21st International Symposium on Atmospheric and Ocean Optics: Atmospheric Physics,
edited by G. G. Matvienko, O. A. Romanovskii, Proc. of SPIE Vol. 9680, 96801V
© 2015 SPIE · CCC code: 0277-786X/15/$18 · doi: 10.1117/12.2205761

at the zenith angle θ_s and azimuth angle φ between the direction of ray incidence and the optical axis of the detector. The Earth surface is considered homogeneous and reflecting light by the Lambert law with the preset reflection coefficient k_{refl}.

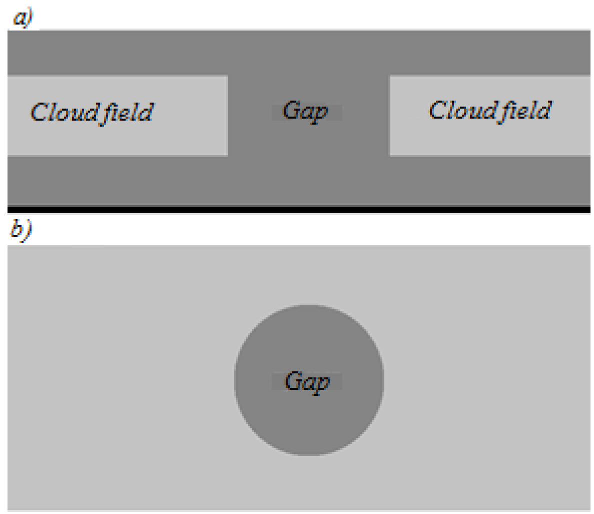

Fig. 1. Gap shape: *a*) cross sectional view; *b*) from the top

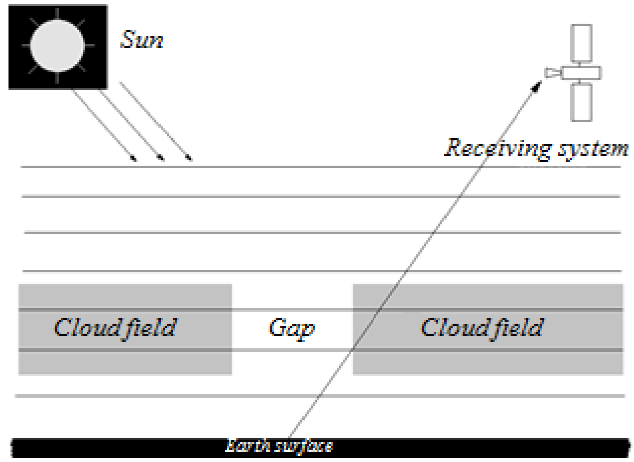

Fig. 2. Geometry of observation

This problem was solved by the Monte Carlo method of numerical simulation based on the scheme of conjugate trajectories of photon wandering. The given simulation technique described in [11] is based on the optical reciprocity principle. Let us consider the case of the absolutely absorbing Earth surface. The vertical boundaries of the cloud layer were assigned at altitudes of 0.5 km and 2.3 km, and the optical cloud parameters were assigned by the generator of optical models based on LOWTRAN-7 [12] (C01 cloud model (cumulus clouds at mid-latitudes in summer) with the optical thickness of the cloud layer $\tau_{cl} = 36$ and the light wavelength $\lambda = 0.55$ μm) with the parameters of the cloudless atmosphere corresponding to the meteorological visibility range $S_M = 50$ km. In this case, we calculated the dependence of the received signal intensity on the gap radius shown in Fig. 3, a and b (they differed only by ranges of values on the abscissa).

The horizontal straight lines show the values calculated for the horizontally homogeneous atmosphere: without clouds (the lower horizontal straight line) and in the presence of continuous cloudiness (the upper horizontal straight line).

The same dependence in the case of a gap sharply decreased where the cloud layer between the point on the Earth surface and the satellite had relatively small optical thickness. This decrease is slowed down significantly when the observation point is seen from the satellite through the gap in the cloud. However, the influence of clouds here does not disappear completely. This is caused by the fact that photons scattered within the cloud can then be scattered again in the region of the gap in the direction toward the receiver. With further increase in the gap radius, the influence of the cloud medium gradually decreases and for a radius of 70 km, decreases to 10 %.

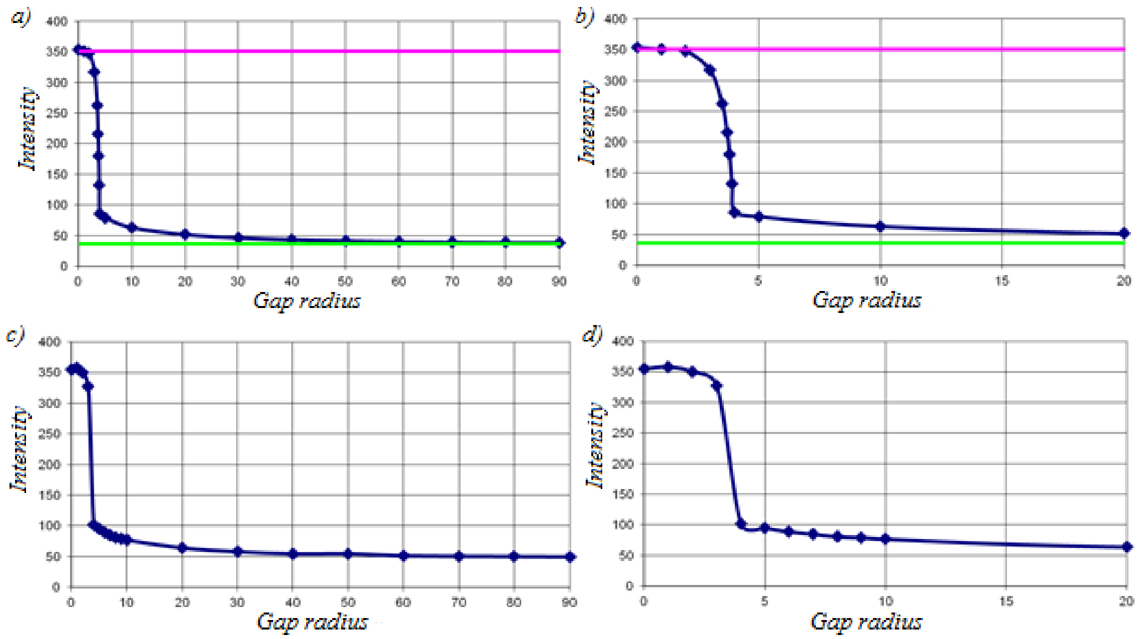

Fig. 3. Dependence of received signal intensity on the gap radius: without reflection from the Earth surface (*a* and *b*) and for the Lambert law of reflection with the coefficient $k_{\text{refl}} = 0.3$. In all cases, the solar zenith angle was $\theta_s = 20°$, the zenith angle of the receiver was $\theta_{\text{rec}} = 60°$, and the azimuth angle was $\varphi = 70°$.

3. SIMULATION OF LIGHT PROPAGATION THROUGH A STOCHASTIC CLOUD FIELD

Above we have considered the case of a single gap in the continuous cloud layer. Meanwhile, such configuration can infrequently be met in actual practice. Much more often one deals with broken cloudiness having many randomly distributed gaps. In this regard, it would be useful to consider the problem of observation of the Earth surface through a gap with a stochastic cloud field outside.

Such problems — problems of solving the radiative transfer equation (RTE) in stochastic media — are often meet in atmospheric and oceanic optics. Therefore, to solve this problem, the mathematical apparatus has been developed, including both direct simulation by the Monte Carlo method (for example, see [13–15]) and G. A. Titov's method of approximate solution of the average RTE — the method of closed equations (see Chapters 7 and 8 in [16]). Results of computations by these methods were considered in [17–19]. Before we proceed directly to a solution of the problem of interest to us, it would be useful to compare these two methods to choose less labor-consuming and to estimate the accuracy of approximate solutions.

For a comparison, we consider one of the simplest models of the stochastic medium, namely, the flat model of the *cloud field* bounded by altitudes h and H and consisting of rectangular *clouds* (see Section 6.2.3 in [16]).

For each trajectory, special realization of the cloud field was generated as follows. The rectangle 25 × 25 km was taken. The flow of points was constructed on each coordinate axis: the distance from 0 to 25 km was subdivided into smaller 250 subsections 100 m long (this distance corresponds to the accuracy of determination of the cloud boundary); in each of these small subsections, the presence or absence of a point was modeled according to the Poisson distribution (if a random number is less than $\lambda e^{-\lambda}$ — the point is present; if it is greater — the point is absent, where $\lambda = (25/D - 1)/250$, $D = 1$ km is the average horizontal size of the cloud). Every possible pairs of these points (x, y) mark the apexes of rectangles into which the initial regions is subdivided. For each of these rectangles, the presence (or absence) of *cloudy substance* in it is simulated: if the random number is less than a certain value (*the cloud cover index*) — the cloudy substance is present, if it is greater — the cloudy substance is absent. After that 25 × 25 km rectangles filled the entire horizontal plane (the entire cloud layer).

The Earth surface was considered absolutely absorbing. All cloud parameters and observation geometry (except for the geometry of the cloud field) remained the same as in Section 1. The cloudless atmosphere was considered absolutely transparent (the method of the closed equations was developed only for this case).

To directly simulate the free path length, the method of the maximum cross section was used (see Section 2.3 of [11]). It is the most efficient method for complex media, and from each collision point, the local estimate to the receiver was carried out. The computation of this local estimate was complicated by the fact that some part of the distance from the scattering point to the receiver light propagated within the cloud, and another part it propagated out of the cloud; moreover, multiple crossing of cloud boundaries by light was also possible. For each photon trajectory, the intensity of radiation arriving at the receiver was calculated; then averaging over all trajectories was performed (in our computations we considered from 150 000 to 1 500 000 photon trajectories for each set of the input parameters in different cases). Similar procedures were described in [13–15].

For simulation by G. A. Titov's method, the stochastic cloud field was replaced by a fictitious homogeneous medium. In this case, the Markov chain was determined by the initial probability density

$$\Psi(\boldsymbol{x}) = \sum_{i=1}^{2} C_i \, \lambda_i e^{-\lambda_i |\boldsymbol{r}-\boldsymbol{r}_H|} \delta(\boldsymbol{\omega} - \boldsymbol{\omega}_{sun}) \qquad (1)$$

and by the transition probability density $k(\boldsymbol{x}', \boldsymbol{x})/\lambda$, where $k(\boldsymbol{x}', \boldsymbol{x})$ is the substochastic kernel (see pp. 155 and 156 of [16,]):

$$k(\boldsymbol{x}', \boldsymbol{x}) = \frac{\lambda g(\mu) \sum_{i=1}^{2} D_i \lambda_i e^{-\lambda_i |\boldsymbol{r}-\boldsymbol{r}'|}}{2\pi |\boldsymbol{r}-\boldsymbol{r}'|^2} \delta\left(\frac{\boldsymbol{r}-\boldsymbol{r}'}{|\boldsymbol{r}-\boldsymbol{r}'|} - \boldsymbol{\omega}\right), \qquad (2)$$

where $\boldsymbol{x} = (x, y, z, a, b, c)$ is the 6-vector of coordinates and directions, $\boldsymbol{\omega} = (a, b, c)$ specifies the direction of radiation propagation, $\boldsymbol{\omega}_{\text{sun}}$ is the direction of incidence of solar rays,

$$C_1 = \frac{\lambda_2 - \sigma p}{\lambda_2 - \lambda_1}, \quad C_2 = 1 - C_1, \quad D_1 = \frac{\lambda_2 - \sigma}{\lambda_2 - \lambda_1}, \quad D_2 = \frac{\sigma - \lambda_1}{\lambda_2 - \lambda_1}, \qquad (3)$$

$$\lambda_{1,2} = \frac{\sigma + A(\omega)}{2} \mp \frac{\sqrt{[\sigma + A(\omega)]^2 - 4A(\omega) p \sigma}}{2}, \quad A(\boldsymbol{\omega}) = (|a| + |b|)[1{,}65(p - 0{,}5)^2 + 1{,}04]/D, \qquad (4)$$

p is the cloud cover index ($0 \le p \le 1$), σ is the light extinction coefficient in the cloud, λ is the quantum survival probability in collision, $\boldsymbol{r}_H$ is a point belonging to the plane $z = H$, D is the average cloud size (we considered $D = 1$ km), $g(\mu)$ is the scattering phase function, and μ is the cosine of the scattering angle. Then the local estimate of radiation received by the satellite system was calculated with allowance for the fact that *the optical path length* in the fictitious homogeneous medium was $\tau = -\lambda_2 \left|\frac{H-z}{\cos\theta_{\text{res}}}\right|$ (z is the altitude of the scattering point).

We considered 1 500 000 trajectories for each set of the input parameters in the case of simulation by this method (as well as for the homogeneous atmosphere).

We start our analysis of the result obtained from the fact that for continuous cloudiness, the results of computations by all three methods coincided (they differed within the statistical error). Figure 4 shows the results of simulation by the competing methods of the intensity of radiation transmitted through the broken cloudiness at the observation point.
From the results shown in Fig. 4 it can be seen that differences can reach 20–30 %, and for small cloud cover index they can reach 50 % (the computational error did not exceed 3 %).

At the same time, there were cases when differences were not so significant: in Fig. 1, d they do not exceed 20 %, and in Fig. 1, c they do not exceed 6 %. Unfortunately, we failed to establish a law that would allow us to predict the accuracy of approximate solutions for a given set of optical-geometrical conditions of observation.

The exponential approximation of the conditional probability of the cloud presence at a certain point given that the cloud was present at the given point applied in (p. 144 of [16]) to derive formulas (1)–(4) could be the reason of the given difference. At the same time, though there are some restrictions on the applicability of G. A. Titov's method of closed equations, it allows one to obtain the results close in values to the true data with saving of the computational time (of the order of several hundred times).

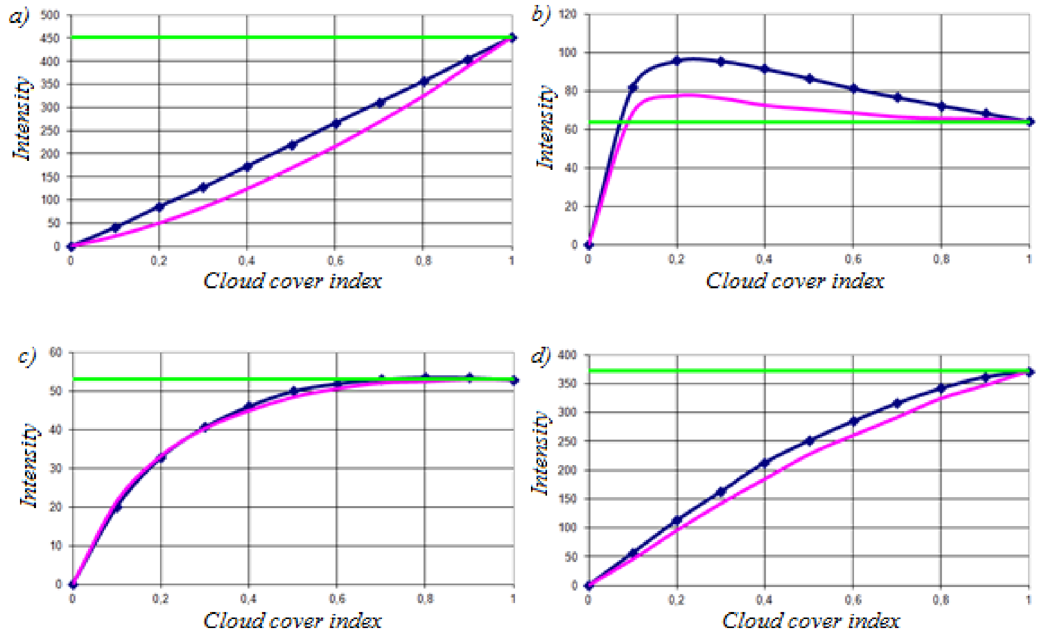

Fig. 4. Comparison of the calculated results: *a*) solar zenith angle $\theta_s = 1^\circ$, zenith angle of the receiver $\theta_{rec} = 30^\circ$, and azimuth angle $\varphi = 70^\circ$; *b*) $\theta_s = 80^\circ$, $\theta_{rec} = 80^\circ$, and $\varphi = 70^\circ$; *c*) $\theta_s = 80^\circ$, $\theta_{rec} = 30^\circ$, and $\varphi = 70^\circ$; *d*) $\theta_s = 1^\circ$, $\theta_{rec} = 70^\circ$, and $\varphi = 70^\circ$. Here curve *1* was calculated by the program of direct simulation of the cloud field, curve 2 was calculated by Titov's method, and curve *3* was calculated for continuous cloudiness by the program for the homogeneous atmosphere.

4. CONCLUSIONS

Our investigations have allowed us to conclude that with increasing gap radius, the intensity changed with non-constant rate: in the beginning, it slowly decreased; then it decreased sharply when the optical path length inside of the cloud became small; after that, the decrease is slowed down again when the observation point became visible through the gap directly. In addition, in the presence of significant reflection from the Earth surface, the dependence of the intensity on the gap radius has a maximum caused in our opinion by the opposite effects of two factors: solar light scattering by clouds (including in the direction toward the receiver) and blocking of light reflected from the Earth surface by these clouds.

A comparison of G. A. Titov's algorithm with the algorithm of direct simulation demonstrated that the difference in some cases remained within 10 %, but can reach 30 %, and can be even 50 % for small cloud cover index (0.1–0.3), which was most likely due to the exponential approximation of the conditional probability of cloud presence at a certain point given that the cloud was already present at the preset point. At the same time, G. A. Titov's method allowed the results close in values to the true data to be obtained while decreasing the computational time several hundred times.

In future we plan to generalize our considerations to the case of observation of the Earth surface through a gap in a cloudy field in the presence of other randomly localized gaps. Estimation of the region of influence of cloudy fields on the image of the Earth surface will allow us to subdivide the satellite image of the Earth surface into cloudless fragments with weak influence of cloudiness where algorithms similar to those presented in [20] can be used, cloudless fragments with significant influence of cloudiness, fragments with translucent cloudiness, and fragments with continuous dense cloudiness.

This work was supported in part by the Russian Foundation for Basic Research (grants Nos. 15-01-00783-A and 15-07-06811-A), by the President of the Russian Federation within the Program for Support of Leading Scientific Schools NSH-4714.2014.5, by the Tomsk State University Academician D. I. Mendeleev Fund Program No. 8.1.27.2015 for 2015, and by the Program of Improving TSU's International Competitiveness for 2013–2020.

REFERENCES

[1] Bartalev, S. A., Lupyan, E. A., Stytsenko, F. V., Panov, O. Yu., Efremov V. Yu., "Express mapping of damages of Russian forests by fires from Landsat satellite data," Sovr. Probl. Dist. Zond. Zemli iz Kosm. Papers 11(1), 9–20 (2014).

[2] Tolpin, V. A., Loupian, E. A., Bartalev, S. A., Plotnikov, D. E., Matveev, A. M., "Possibilities of agricultural vegetation condition analysis with the "VEGA" satellite service," Atmos. Oceanic Optics. Papers 27(7), 581–586 (2014).

[3] Malakhov, D. V., Islamgulova A. F., "The quantitative interpretation of pasture image parameters: An experience of low and moderate spatial resolution remotely sensed data application," Atmos. Oceanic Optics. Papers 27(7), 587–592 (2014).

[4] Kozoderov, V. V., Dmitriev, E. V., Kamentsev V. P., "Cognitive technologies for processing optical images of high spatial and spectral resolution," Atmos. Oceanic Optics. Papers 27(7), 593–600 (2014).

[5] Dagurov, P. N., Dmitriev, A. V., Dymbrylov, Zh. B., Radnaeva S. B., "Earth's surface brightness temperature measured by the microwave radiometer SMOS, and the problem of soil moisture recovering," Atmos. Oceanic Optics. Papers 27(7), 605–609 (2014).

[6] Chimitdorzhiev, T. N., Kirbizhekova, I. I., Bykov. M. E., "Study of landslide processes and deformations of the landscape of the Yamal peninsula by radar interferometry and texture analysis," Atmos. Oceanic Optics. Papers 27(7), 610–614 (2014).

[7] Tomshin, O. A., Solovyev V. S., "Studying of variations of atmospheric aerosol properties caused by large-scale forest fires in Central Yakutia (2002)," Atmos. Oceanic Optics. Papers 27(7), 634–639 (2014).

[8] Polishchuk, Yu. M., Tokareva O. S., "The use of satellite images for ecological estimate of flare firing of gas at oil fields of Siberia," Atmos. Oceanic Optics. Papers 27(7), 647–651 (2014).

[9] Kataev, M. Yu., Bekerov A. A., "Detection of ecological changes in the natural medium from satellite measurements," Atmos. Oceanic Optics. Papers 27(7), 652–656 (2014).

[10] Solomatov, D. V., Afonin, S. V., Belov V. V., "Construction of cloud mask and removal of semitransparent clouds on ETM +/Landsat-7 satellite images," Atmos. Oceanic Optics. Papers 26(9), 798–803 (2013).

[11] Marchuk, G. I., Mikhailov, G. A., Nazaraliev, M. A., Darbinyan, R. A., Kargin, B. A., Elepov, B. S., [Monte Carlo Method in Atmospheric Optics], Nauka, Siberian Branch, Novosibirsk, 284 (1976).

[12] Kneizys, F. X., Shettle, E. P., Anderson, G. P., Abreu, L. W., Chetwynd, J. H., Selby, J. E. A., Clough, S. A., Gallery, W. O., [User Guide to LOWTRAN-7. ARGL-TR-86-0177.ERP 2010], Hansom AFB, MA 01731, 137.

[13] Prigarin, S. M., Zhuravleva, T. B., Volikova, P. V., "Poisson model of multilayer broken clouds," Atmos. Oceanic Optics. Papers 15(10), 917–924 (2002).

[14] Kargin, B. A., Prigarin, S. M., "Simulation of heap clouds for investigation of solar radiation transfer processes by Monte Carlo method," Atmos. Oceanic Optics. Papers 7(9), 1275–1287 (1994).

[15] Prigarin, S. M., Kargin, B. A., Oppel, U. G., "Random fields of broken clouds and their associated direct solar radiation, scattered transmission, and albedo," Pure Appl. Opt. Papers 7(6), 1389–1402 (1998).

[16] Zuev, V. E., Titov, G. A., [Atmospheric Optics and Climate], Spectrum Publishing House, Tomsk, 272 (1996).

[17] Titov, G. A., Zhuravleva, T. B., Zuev, V. E., "Mean radiation fluxes in the near-IR spectal range: Algorithms for calculation," J. Geophys. Res. Papers 102(D2), 1819–1832 (1997).

[18] Zhuravleva, T. B., Firsov, K. M., "Algorithms for calculation of sunlight fluxes in the cloudy and cloudless atmosphere," Atmos. Oceanic Optics. Papers 17(11), 903–911 (2004).

[19] Zhuravleva, T. B. "Simulation of solar radiative transfer under different atmospheric conditions. Part II: Stochastic clouds," Atm. Oceanic Optics. Papers 21(3), 189–202 (2008).

[20] Tarasenkov, M. V., Belov V. V., "Software package for reconstruction of reflective properties of the Earth surface in visible and UV ranges," Atmos. Oceanic Optics. Papers 27(7), 622–627 (2014).